Title
Permeability imaging as a predictor of delayed cerebral ischemia after aneurysmal subarachnoid hemorrhage

Journal
Cerebrovascular and Brain Metabolism Reviews, 38(6)

ISSN
1040-8827

Authors
Russin, Jonathan J
Montagne, Axel
D'Amore, Francesco
et al.

Publication Date
2018-06-01

DOI
10.1177/0271678x18768670

Brief Communication

JCBFM

Journal of Cerebral Blood Flow & Metabolism
2018, Vol. 38(6) 973–979

DOI: 10.1177/0271678X18768670
journals.sagepub.com/home/jcbfm
SAGE

Permeability imaging as a predictor of delayed cerebral ischemia after aneurysmal subarachnoid hemorrhage

Jonathan J Russin[1,4], Axel Montagne[2], Francesco D'Amore[3], Shuhan He[2], Mark S Shiroishi[3], Robert C Rennert[1], Jena Depetris[2], Berislav V Zlokovic[2] and William J Mack[2,4]

Abstract

Blood–brain barrier (BBB) dysfunction has been implicated in ischemic risk following aneurysmal subarachnoid hemorrhage (aSAH), but never directly imaged. We prospectively examined whether post-bleed day 4 dynamic contrast-enhanced magnetic resonance (DCE-MR) BBB permeability imaging could predict development of delayed cerebral ischemia (DCI). Global MR-derived BBB permeability (K_{trans}) was significantly higher in aSAH patients who subsequently developed DCI (five patients; $2.28 \pm 0.09 \times 10^{-3}$ min^{-1}) compared to those who experienced radiographic vasospasm only (three patients; $1.85 \pm 0.12 \times 10^{-3}$ min^{-1}; $p < 0.05$), or no vasospasm/ischemia (eight patients; $1.74 \pm 0.07 \times 10^{-3}$ min^{-1}; $p < 0.01$). $K_{trans} > 2 \times 10^{-3}$ min^{-1} predicted development of DCI (AUC = 0.98, 95% CI: 0.93–1). Global BBB dysfunction following aSAH is detectable with DCE-MR and predictive of ischemic risk.

Keywords

Delayed cerebral ischemia, subarachnoid hemorrhage, dynamic contrast-enhanced magnetic resonance imaging, aneurysm, blood–brain barrier

Received 26 December 2017; Revised 3 February 2018; Accepted 6 March 2018

Introduction

Delayed cerebral ischemia (DCI) is a multifactorial process often concomitant with radiographic cerebral vasospasm that occurs in approximately 30% of patients after aneurysmal subarachnoid hemorrhage (aSAH).[1,2] Neurological deficits from DCI account for the majority of in-hospital morbidity and mortality in aSAH patients, and dramatically impact functional outcomes. Prospective identification of those patients at highest risk for DCI following aSAH is nonetheless challenging, as current assessments of ischemic risk are largely based on crude measures of subarachnoid blood,[3–5] and radiographic vasospasm can occur with or without clinical or ischemic sequelea.[6]

While the exact mechanisms underlying cerebral vasospasm and DCI following aSAH remain poorly understood, the importance of early microvascular dysfunction and the inflammatory response in these processes has been established in laboratory, translational, and clinical models.[7–15] Under normal homeostatic conditions, the brain is a largely immune-privileged organ due to the presence of vascular endothelial cell tight-junctions comprising the blood–brain barrier (BBB). Following aSAH, pathologic extravasation of leukocytes through the BBB microvasculature leads to

[1]USC Neurorestoration Center, Keck School of Medicine, University of Southern California, Los Angeles, CA, USA
[2]Zilkha Neurogenetic Institute, Keck School of Medicine, University of Southern California, Los Angeles, CA, USA
[3]Department of Radiology, Keck School of Medicine, University of Southern California, Los Angeles, CA, USA
[4]Department of Neurological Surgery, Keck School of Medicine, University of Southern California, Los Angeles, CA, USA

The first two authors contributed equally to this work

Corresponding author:
Jonathan J Russin, USC Neurorestoration Center, Keck School of Medicine, University of Southern California, 1200 N State Street, Suite 3300, Los Angeles, CA 90033, USA.
Email: jonathan.russin@med.usc.edu

an upregulation of extravascular inflammatory mediators, the scale of which is proportional to vasospasm and DCI risk.[10,13] BBB dysfunction has also been directly linked to DCI risk through serum elevations of basal membrane catalytic enzymes such as matrix metalloproteinases (MMPs).[16–18] Together, these data suggest that high-resolution imaging of BBB permeability could act as a novel predictor of DCI following aSAH.

In this study, we assess the ability of advanced dynamic contrast-enhanced magnetic resonance (DCE-MR) permeability imaging,[19,20] to identify early and subtle BBB changes following aSAH and prospectively predict risk of DCI.

Materials and methods

This study was approved by and conducted in accordance with the ethical standards of the Institutional Review Board (IRB) of the University of Southern California, and performed in compliance with Health Insurance Portability and Accountability Act regulations. Patient consent for procedures, data collection and review was obtained based on institutional guidelines. Data on consecutive patients presenting with aSAH were collected. In addition to standard aSAH care (detailed in the Supplemental Materials and Methods), a DCE-MR scan on post-bleed day (PBD) 4 (prior to the day 7 peak vasospasm period)[21] was obtained. Patients were screened daily for vasospasm using transcranial Doppler (TCD) ultrasonography, and those with elevated TCDs or neurologic declines underwent computed tomographic angiography (CTA) to assess for radiographic vasospasm.

Primary study outcome was development of DCI (defined as a new onset focal neurologic deficit with radiographic vessel narrowing without other pathologic explanations) within 14 days of aSAH. Patients were classified into three groups based on clinical course: no vasospasm or ischemia, radiographic vasospasm only, and DCI, with MR-derived BBB permeability compared across groups.

DCE-MR imaging

DCE-MR images were obtained and processed as detailed in the Supplemental Materials and Methods. Briefly, user defined regions-of-interest (ROIs) were placed in standardized representative vascular territories (Figure 1). Patlak linear regression analysis with individual vascular input functions was used for voxel-by-voxel calculation of the BBB transfer constant between blood plasma and the extravascular extracellular space (K_{trans}), volume of the extravascular extracellular space per unit volume of tissue (v_e), and fractional plasma volume (v_p).

Data analysis

See Supplemental Materials and Methods for full data analysis. Briefly, data normality was assessed using a scatter plot and Anderson–Darling test. The random effect model was used to assess inter-group and inter-ROI variations and interactions, prior to post hoc contrast or ANOVA testing. Hochberg's step-up procedure was used for correction of multiple testing errors. Receiver operating characteristic (ROC) curves were used to assess the discrimination power of DCE-MR to predict DCI. SAS9.4 software (SAS Institute, Cary, NC) was used for all data analysis. An alpha level of 0.05 was used as the experimental wise error.

Results

Baseline patient data and vasospasm outcomes

Twenty patients presenting with aSAH were enrolled, with sixteen patients included in the final analysis (four excluded due to insufficient imaging quality). Of these 16 patients, 5 were male and 11 were female; average age was 57.6 ± 12.2 years. Hunt Hess (HH) scores ranged from 2 to 5 (average of 3.3) and Fisher scores ranged from 2 to 4 (average of 3.6). The most common aneurysm location was the anterior communicating artery (Acomm) region (6), followed by the middle cerebral artery (MCA) (4), posterior communicating artery (Pcomm) (3), posterior inferior cerebellar artery (PICA), vertebral artery (2), and ophthalmic artery (1). Nine of 16 patients underwent coiling for aneurysm treatment, with seven patients undergoing craniotomy for aneurysm clipping (Table 1). Five patients developed DCI, three developed radiographic only vasospasm, and eight did not develop vasospasm or ischemia.

DCE-MR predicts clinical vasospasm

Three DCE-MR parameters were assessed. A statistically significant intersubject variability in the volume of the extravascular extracellular space per unit volume of tissue (v_e), and fractional plasma volume (v_p) was not observed. K_{trans} values from each ROI were analyzed to identify potential differences in BBB permeability between ROIs and clinical groups (Figure 1(a) to (d), Supplemental Table 1). The random effect model did not show a significant interaction between clinical groups and ROIs ($p = 0.19$ with original data, $p = 0.22$ with Wilcoxon ranking score transformation), indicating that any differences across groups were consistent for all ROIs. Intrasubject ROIs were averaged prior to further analysis.

Average DCE-MR K_{trans} values demonstrated significant intergroup differences ($p < 0.01$ on global ANOVA).

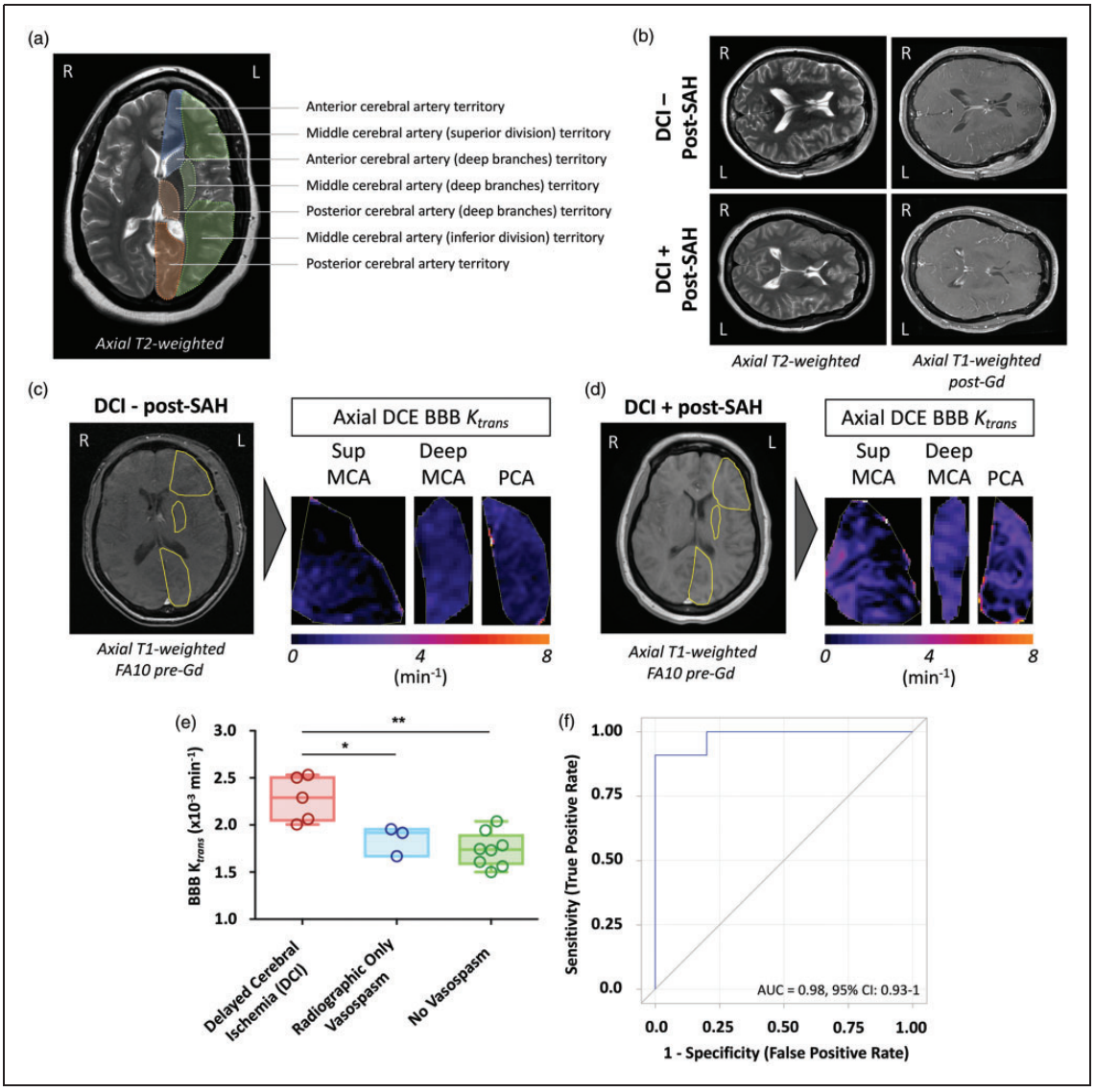

Figure 1. DCE-MR blood–brain barrier imaging (K_{trans}) as a predictor of DCI. Standardized ROIs are shown (a) with labels of the vascular territory they represent. No significant differences can be appreciated using standard imaging protocols (b). Representative ROIs from a case without DCI (c) and with DCI (d) illustrate differences in DCE-MR BBB K_{trans} values. (e) Following intrasubject ROI averaging, PBD 4 BBB K_{trans} values were significantly higher in patients who developed DCI compared to those who developed radiographic only or no vasospasm/ischemia. (f) DCE-MR ROC curves accurately predicted patients who developed DCI from those who experienced radiographic only and no vasospasm/ischemia. * indicates $p < 0.05$; **$p < 0.01$.

Pair-wise intergroup analysis demonstrated that patients with DCI had significantly higher K_{trans} values ($2.28 \pm 0.09 \times 10^{-3}$ min^{-1}) compared to patients with radiographic only ($1.85 \pm 0.12 \times 10^{-3}$ min^{-1}; $p < 0.05$), or no vasospasm/ischemia ($1.74 \pm 0.07 \times 10^{-3}$ min^{-1}; $p < 0.01$) (Figure 1(e)). ROC curve analysis demonstrated that DCE-MR accurately predicted patients who developed DCI from those who experienced radiographic only or no vasospasm/ischemia (AUC = 0.98, 95% CI: 0.93–1; diagnostic cut point 2×10^{-3} min^{-1}) (Figure 1(f)).

Discussion

The link between BBB permeability and DCI following aSAH has been explored in previous works, but not directly imaged. The first step in this process, microvascular dysfunction, begins immediately after aSAH and includes pathologic vasoconstriction, luminal platelet aggregation, and activation of early inflammatory cascades.[14,15] Increased BBB permeability also occurs within 24 h post-hemorrhage as a result of endothelial dysfunction from oxidative stress and structural

Table 1. Baseline patient data and clinical outcomes.

Patient #	Age	Sex	Race	Aneurysm location	SAH Grade	Aneurysm treatment	Radiographic spasm	DCI	PBD for DCI	Stroke related to DCI
1	55	F	H/L	L PComm	HH2F2	Coiling	No	No	x	No
2	73	M	Cauc	R A1/2 jxn	HHFF4	Coiling	No	No	x	No
3	47	F	AA	Acomm	HH3F4	Coiling	Yes	Yes	7	Yes - b/l ACA
4	52	F	Cauc	L MCA	HH3F4	Clipping	No	No	x	No
5	40	F	AA	R Pcomm and R Ant Choroidal	HH2F3	Coiling x 2	No	No	x	No
6	50	F	AA	L MCA	HH2F4	Clipping	Yes	Yes	5	Yes- L MCA and L MCA/ACA watershed
7	76	F	H/L	R MCA	HH3F4	Clipping	No	No	x	No
8	51	M	Asian	L Vert	HH3F4	Coiling	No	No	x	No
9	52	F	H/L	R PICA	HH4F4	Clipping	Yes	No	x	No
10	73	F	H/L	R MCA	HH5F4	Clipping	Yes	No	x	No
11	47	M	Cauc	Acomm	HH2F4	Clipping	Yes	Yes	9	No
12	53	M	Cauc	L A1/2 jxn	HH5F4	Coiling	Yes	yes	4	No
13	52	F	AA	L Oph	HH4F4	Coiling	Yes	Yes	7	Yes- L MCA/ACA watershed
14	56	M	H/L	Acomm	HH2F2	Clipping	No	No	x	No
15	83	F	Asian	R Pcomm	HH3F3	Coiling	No	No	x	No
16	63	F	Cauc	R A1/2 jxn	HH5F4	Coiling	Yes	No	x	No

AA: African American; Acomm: anterior communicating artery; ACA: anterior cerebral artery; Cauc: Caucasian; MCA: middle cerebral artery; F: female; H/L: hispanic/latino; HH/F: hunt Hess/Fisher scales; M: male; Oph: ophthalmic artery; Pcomm: posterior communicating artery; PICA: posterior inferior cerebellar artery; Vert: vertebral artery.

breakdown, as well as basal lamina degradation.[14,15] These BBB alterations allow migration of macrophages and neutrophils into the subarachnoid space to 'clean up' extraluminal red blood cells as they begin to undergo hemolysis.[22–31] There is no recognized pathway for these leukocytes to return to the circulation, however, and after approximately two to four days, they begin to undergo apoptosis.[32] These combined events promote the release of pro-inflammatory and vascular endothelial cell-derived spasmogenic molecules, including intercellular adhesion molecule-1 (ICAM-1), endothelin 1, and E-selectin, and are thought to contribute to the development of large-vessel vasospasm and DCI.[8,33–36]

While it is therefore logical that existing DCI risk scales are largely based on aSAH blood volumes,[3–5,37] which should be proportional to the resulting inflammatory response, these scales have relatively poor predictive value. Several molecules have nonetheless linked BBB disruption following aSAH directly to DCI risk, suggesting the BBB as a potentially more clinically predictive target than SAH volume. MMPs released by microglia, astrocytes, and endothelial cells in the brain during extracellular matrix remodeling are one such molecule and have been previously identified as contributing to inflammatory conditions in the nervous system.[38] Multiple clinical studies measuring circulating soluble MMPs following sSAH have also demonstrated significantly higher MMP levels (specifically MMP-9) prior to the development of DCI.[17,18] Additionally, in animal models of SAH, downregulation of MMP-9 expression has been shown to decrease the incidence of cerebral ischemia,[39] consistent with a contributory role of BBB dysfunction in DCI. Several other factors have also been implicated in BBB dysfunction after aSAH, including vascular endothelial growth factor, mitogen-activated protein kinase, hypoxia-inducible factor-1α, von Willebrand factor, and the upregulation of aquaporins,[17,40–43] some of which have been linked to DCI risk.

Building on these works, we hypothesized that global changes in the BBB, if measurable, should be more pronounced in patients that experience DCI versus those who do not. Our data support this hypothesis, as DCE-MR permeability did not vary significantly among ROIs in the same patient, but still predicted the development of DCI as compared to radiographic vasospasm only or no vasospasm/ischemia. These findings are also consistent with the increasing recognition of the complex global vascular pathophysiologic processes

that separate DCI from asymptomatic, 'mechanical' large-vessel narrowing.[44] Although our data differ subtly from a recently published study linking focal rather than global computed tomography perfusion (CTP) changes (an indirect marker of BBB dysfunction) with DCI,[45] this retrospective analysis used only regional in-patient controls and did not assess CTP in patients with radiographic vasospasm only or no vasospasm/ischemia, limiting the interpretation and clinical utility of this work.

Mechanistically, while it is unclear whether the early BBB dysfunction characterized by DCE-MR plays a causal role in subsequent DCI development, or is itself a concomitant marker of more influential upstream microcirculatory pathologic processes, the ability of BBB modulating agents to affect DCI risk suggests at least some causality between these processes.[39] As the previously identified serum markers of vasospasm risk only indirectly assess BBB permeability,[17,18] the ability to directly assess global BBB permeability changes that predict DCI risk via non-invasive DCE-MR represents a major advancement for aSAH research. Moreover, because DCE-MR imaging was completed on PBD 4, correlating with peak levels of circulating biomarkers associated with BBB dysfunction but preceding the highest DCI risk period,[17,18,21] these data provide a clinically relevant window for potential alterations in the management of high-risk aSAH patients in future studies.

Despite the relatively small sample size of our study, its prospective design allowed for robust statistical analyses to determine not only a significant correlation between DCE-MR and DCI, but also the discrimination power of this imaging modality using ROC curves. With a statistical power comparable to several recent reports assessing other imaging modalities after aSAH,[45–48] our data highlight the clear clinical potential of MR permeability testing after aSAH. Future, larger studies will nonetheless be needed to confirm the findings of this pilot work.

Conclusion

BBB MR-permeability imaging can accurately identify patients at highest risk for developing DCI following aSAH.

Funding

Brain Aneurysm Foundation Carol Harvey Memorial Grant; NIH ES024936 WJM; NIH #AG 052350 and Leducq Foundation #16 CVD 05 BVZ; KLFTR000131 MSS.

Acknowledgements

The authors thank Dr. Steven Cen for his assistance with statistical analysis for this work.

Declaration of conflicting interests

The author(s) declared no potential conflicts of interest with respect to the research, authorship, and/or publication of this article.

Authors' contributions

JJR and WJM contributed to the study concept and design. JJR, AM, FD, SH, MSS, RCR, JD, BVZ and WJM contributed to data acquisition, analysis, and interpretation of data, and/or manuscript drafting/critical revising for intellectual content. All authors approved the submitted version of the manuscript to be published.

Supplementary material

Supplementary material for this paper can be found at the journal website: http://journals.sagepub.com/home/jcb

ORCID iD

Jena Depetris http://orcid.org/0000-0002-2544-7496

References

1. Dorsch N. A clinical review of cerebral vasospasm and delayed ischaemia following aneurysm rupture. *Acta Neurochir Suppl* 2011; 110(Pt 1): 5–6.
2. Vergouwen MD, Vermeulen M, van Gijn J, et al. Definition of delayed cerebral ischemia after aneurysmal subarachnoid hemorrhage as an outcome event in clinical trials and observational studies: proposal of a multidisciplinary research group. *Stroke* 2010; 41: 2391–2395.
3. Claassen J, Bernardini GL, Kreiter K, et al. Effect of cisternal and ventricular blood on risk of delayed cerebral ischemia after subarachnoid hemorrhage: the Fisher scale revisited. *Stroke* 2001; 32: 2012–2020.
4. Fisher CM, Kistler JP and Davis JM. Relation of cerebral vasospasm to subarachnoid hemorrhage visualized by computerized tomographic scanning. *Neurosurgery* 1980; 6: 1–9.
5. Frontera JA, Claassen J, Schmidt JM, et al. Prediction of symptomatic vasospasm after subarachnoid hemorrhage: the modified fisher scale. *Neurosurgery* 2006; 59: 21–27; discussion 21–27.
6. Vergouwen MD, Ilodigwe D and Macdonald RL. Cerebral infarction after subarachnoid hemorrhage contributes to poor outcome by vasospasm-dependent and -independent effects. *Stroke* 2011; 42: 924–929.
7. Al-Tamimi YZ, Orsi NM, Quinn AC, et al. A review of delayed ischemic neurologic deficit following aneurysmal subarachnoid hemorrhage: historical overview, current treatment, and pathophysiology. *World Neurosurg* 2010; 73: 654–667.
8. Chaichana KL, Pradilla G, Huang J, et al. Role of inflammation (leukocyte-endothelial cell interactions) in vasospasm after subarachnoid hemorrhage. *World Neurosurg* 2010; 73: 22–41.
9. Chang CZ, Dumont AS, Simsek S, et al. The adenosine 2A receptor agonist ATL-146e attenuates experimental

posthemorrhagic vasospasm. *Neurosurgery* 2007; 60: 1110–1117; discussion 1117–1118.
10. Dhar R and Diringer MN. The burden of the systemic inflammatory response predicts vasospasm and outcome after subarachnoid hemorrhage. *Neurocrit Care* 2008; 8: 404–412.
11. Iseda K, Ono S, Onoda K, et al. Antivasospastic and antiinflammatory effects of caspase inhibitor in experimental subarachnoid hemorrhage. *J Neurosurg* 2007; 107: 128–135.
12. Lin CL, Kwan AL, Dumont AS, et al. Attenuation of experimental subarachnoid hemorrhage-induced increases in circulating intercellular adhesion molecule-1 and cerebral vasospasm by the endothelin-converting enzyme inhibitor CGS 26303. *J Neurosurg* 2007; 106: 442–448.
13. Provencio JJ, Fu X, Siu A, et al. CSF neutrophils are implicated in the development of vasospasm in subarachnoid hemorrhage. *Neurocrit Care* 2010; 12: 244–251.
14. Sehba FA and Friedrich V. Early micro vascular changes after subarachnoid hemorrhage. *Acta Neurochir Suppl* 2011; 110(Pt 1): 49–55.
15. Tso MK and Macdonald RL. Acute microvascular changes after subarachnoid hemorrhage and transient global cerebral ischemia. *Stroke Res Treat* 2013; 2013: 425281.
16. Akpinar A, Ucler N, Erdogan U, et al. Measuring serum matrix metalloproteinase-9 levels in peripheral blood after subarachnoid hemorrhage to predict cerebral vasospasm. *Springerplus* 2016; 5: 1153.
17. McGirt MJ, Lynch JR, Blessing R, et al. Serum von Willebrand factor, matrix metalloproteinase-9, and vascular endothelial growth factor levels predict the onset of cerebral vasospasm after aneurysmal subarachnoid hemorrhage. *Neurosurgery* 2002; 51: 1128–1134; discussion 1134–1135.
18. Fischer M, Dietmann A, Beer R, et al. Differential regulation of matrix-metalloproteinases and their tissue inhibitors in patients with aneurysmal subarachnoid hemorrhage. *PLoS One* 2013; 8: e59952.
19. Montagne A, Barnes SR, Sweeney MD, et al. Blood-brain barrier breakdown in the aging human hippocampus. *Neuron* 2015; 85: 296–302.
20. Barnes SR, Ng TS, Montagne A, et al. Optimal acquisition and modeling parameters for accurate assessment of low Ktrans blood-brain barrier permeability using dynamic contrast-enhanced MRI. *Magn Reson Med* 2016; 75: 1967–1977.
21. Weir B, Grace M, Hansen J, et al. Time course of vasospasm in man. *J Neurosurg* 1978; 48: 173–178.
22. Doczi T. The pathogenetic and prognostic significance of blood-brain barrier damage at the acute stage of aneurysmal subarachnoid haemorrhage. Clinical and experimental studies. *Acta Neurochir* 1985; 77: 110–132.
23. Doczi T, Joo F, Adam G, et al. Blood-brain barrier damage during the acute stage of subarachnoid hemorrhage, as exemplified by a new animal model. *Neurosurgery* 1986; 18: 733–739.
24. Doczi T, Joo F, Sonkodi S, et al. Increased vulnerability of the blood-brain barrier to experimental subarachnoid hemorrhage in spontaneously hypertensive rats. *Stroke* 1986; 17: 498–501.
25. D'Avella D, Germano A, Santoro G, et al. Effect of experimental subarachnoid hemorrhage on CSF eicosanoids in the rat. *J Neurotrauma* 1990; 7: 121–129.
26. Germano A, d'Avella D, Cicciarello R, et al. Blood-brain barrier permeability changes after experimental subarachnoid hemorrhage. *Neurosurgery* 1992; 30: 882–886.
27. Germano A, d'Avella D, Imperatore C, et al. Time-course of blood-brain barrier permeability changes after experimental subarachnoid haemorrhage. *Acta Neurochir* 2000; 142: 575–580; discussion 580–581.
28. Johshita H, Kassell NF and Sasaki T. Blood-brain barrier disturbance following subarachnoid hemorrhage in rabbits. *Stroke* 1990; 21: 1051–1058.
29. Nakagomi T, Kassell NF, Johshita H, et al. Blood-arterial wall barrier disruption to various sized tracers following subarachnoid haemorrhage. *Acta Neurochir* 1989; 99: 76–84.
30. Nakagomi T, Kassell NF, Sasaki T, et al. Time course of the blood-arterial wall barrier disruption following experimental subarachnoid haemorrhage. *Acta Neurochir* 1989; 98: 176–183.
31. Trojanowski T. Blood-brain barrier changes after experimental subarachnoid haemorrhage. *Acta Neurochir* 1982; 60: 45–54.
32. Pradilla G, Chaichana KL, Hoang S, et al. Inflammation and cerebral vasospasm after subarachnoid hemorrhage. *Neurosurg Clin N Am* 2010; 21: 365–379.
33. Mocco J, Mack WJ, Kim GH, et al. Rise in serum soluble intercellular adhesion molecule-1 levels with vasospasm following aneurysmal subarachnoid hemorrhage. *J Neurosurg* 2002; 97: 537–541.
34. Mack WJ, Mocco J, Hoh DJ, et al. Outcome prediction with serum intercellular adhesion molecule-1 levels after aneurysmal subarachnoid hemorrhage. *J Neurosurg* 2002; 96: 71–75.
35. Lin CL, Dumont AS, Calisaneller T, et al. Monoclonal antibody against E selectin attenuates subarachnoid hemorrhage-induced cerebral vasospasm. *Surg Neurol* 2005; 64: 201–205; discussion 205–206.
36. Pluta RM, Hansen-Schwartz J, Dreier J, et al. Cerebral vasospasm following subarachnoid hemorrhage: time for a new world of thought. *Neurol Res* 2009; 31: 151–158.
37. Fisher CM, Roberson GH and Ojemann RG. Cerebral vasospasm with ruptured saccular aneurysm–the clinical manifestations. *Neurosurgery* 1977; 1: 245–248.
38. Candelario-Jalil E, Yang Y and Rosenberg GA. Diverse roles of matrix metalloproteinases and tissue inhibitors of metalloproteinases in neuroinflammation and cerebral ischemia. *Neuroscience* 2009; 158: 983–994.
39. Maddahi A, Ansar S, Chen Q, et al. Blockade of the MEK/ERK pathway with a raf inhibitor prevents activation of pro-inflammatory mediators in cerebral arteries and reduction in cerebral blood flow after subarachnoid hemorrhage in a rat model. *J Cereb Blood Flow Metab* 2011; 31: 144–154.
40. Terpolilli NA, Brem C, Buhler D, et al. Are We barking up the wrong vessels? cerebral microcirculation after subarachnoid hemorrhage. *Stroke* 2015; 46: 3014–3019.

41. Feiler S, Plesnila N, Thal SC, et al. Contribution of matrix metalloproteinase-9 to cerebral edema and functional outcome following experimental subarachnoid hemorrhage. *Cerebrovasc Dis* 2011; 32: 289–295.
42. Badaut J, Brunet JF, Grollimund L, et al. Aquaporin 1 and aquaporin 4 expression in human brain after subarachnoid hemorrhage and in peritumoral tissue. *Acta Neurochir Suppl* 2003; 86: 495–498.
43. Ostrowski RP, Colohan AR and Zhang JH. Molecular mechanisms of early brain injury after subarachnoid hemorrhage. *Neurol Res* 2006; 28: 399–414.
44. Zhang JH. Vascular neural network in subarachnoid hemorrhage. *Transl Stroke Res* 2014; 5: 423–428.
45. Ivanidze J, Kesavabhotla K, Kallas ON, et al. Evaluating blood-brain barrier permeability in delayed cerebral infarction after aneurysmal subarachnoid hemorrhage. *Am J Neuroradiol* 2015; 36: 850–854.
46. Aralasmak A, Akyuz M, Ozkaynak C, et al. CT angiography and perfusion imaging in patients with subarachnoid hemorrhage: correlation of vasospasm to perfusion abnormality. *Neuroradiology* 2009; 51: 85–93.
47. Wintermark M, Ko NU, Smith WS, et al. Vasospasm after subarachnoid hemorrhage: utility of perfusion CT and CT angiography on diagnosis and management. *Am J Neuroradiol* 2006; 27: 26–34.
48. Dankbaar JW, de Rooij NK, Velthuis BK, et al. Diagnosing delayed cerebral ischemia with different CT modalities in patients with subarachnoid hemorrhage with clinical deterioration. *Stroke* 2009; 40: 3493–3498.